

1 Extreme storms during the last 6,500 years from lagoonal
2 sedimentary archives in Mar Menor (SE SPAIN)

3
4
5
6 Dezileau L. ^{*} ¹, Pérez-Ruzafa A. ², Blanchemanche P. ³, Degeai J.P. ³, Raji O. ^{1,4},
7 Martinez P. ⁵, Marcos C. ² and Von Grafenstein U. ⁶

8
9
10 [1]{Université de Montpellier, Geosciences Montpellier, CNRS, UMR 5243}

11 [2]{Universidad de Murcia, Departamento de Ecología e Hidrología, Regional Campus of International Excellence
12 Campus Mare Nostrum, Murcia 30100, Spain}

13 [3]{Université Montpellier 3, Laboratoire d'Archéologie des Sociétés Méditerranéennes, CNRS, UMR 5140}

14 [4]{Department of Earth Sciences, Université MohammedV-Agdal, Rabat, Morocco}

15 [5]{Université Bordeaux 1, EPOC, CNRS, UMR 5805}

16 [6]{Laboratoire des Sciences du Climat et de l'Environnement, CNRS/CEA, Saclay}

17
18
19 * Correspondence to : laurent.dezileau@gm.univ-montp2.fr
20

21

22 **Abstract**

23 Amongst the most devastating marine catastrophes that can occur in coastal areas, are storms and
24 tsunamis, which may seriously endanger human society. Many such events are known and have
25 been reported for the Mediterranean, a region where high-frequency occurrences of these extreme
26 events coincides with some of the most densely populated coastal areas in the world. In a
27 sediment core from Mar Menor Lagoon (SE Spain), we discovered eight coarse grained layers
28 which document marine incursions during periods of intense storm activity or tsunami events.
29 Based on radiocarbon dating, these extreme events occurred around 5250, 4000, 3600, 3010,
30 2300, 1350, 650 and 80 years cal BP. No comparable events have been observed during the 20th
31 and 21th centuries. The results indicate little likelihood of a tsunami origin for these coarse grained
32 layers, although historical tsunami events are recorded in this region. These periods of surge
33 events seem to coincide with the coldest periods in Europe during the late Holocene, suggesting a
34 control by a climatic mechanism for periods of increased storm activity. Spectral analyses
35 performed on the sand % revealed four major periodicities of 1228 ± 327 , 732 ± 80 , 562 ± 58 , and
36 319 ± 16 yr. Amongst the well-known proxies that have revealed a millennial-scale climate
37 variability during the Holocene, the ice-rafted debris (IRD) indices in North Atlantic developed
38 by Bond et al. (1997, 2001) present a cyclicity of 1470 ± 500 yr, which matches the 1228 ± 327 yr
39 periodicity evidenced in the Mar Menor lagoon, considering the respective uncertainties on the
40 periodicities. Thus, an in-phase storm activity in Western Mediterranean is found with the coldest
41 periods in Europe and to the North Atlantic thermohaline circulation. However, further
42 investigations, such as additional coring, high-resolution coastal imagery, are needed to better

43 constrain the main cause of these multiple-events.

44

45

46

47 Keywords: coastal lagoons, storm, tsunami, Mediterranean Sea, Late Holocene.

48

49

50 1. Introduction

51 In the last century the Mediterranean coastal zones have undergone a considerable development
52 and the coastal disasters incidence has significantly increased. The coastal zones are exposed to
53 flooding and coastal erosion processes, and are highly vulnerable to extreme events, such as
54 storms, cyclones or tsunamis, that can cause significant losses (Seisdedos et al., 2013).

55 Mediterranean intense storms and cyclones are rare meteorological phenomena observed in the
56 Mediterranean Sea. Different climatological and meteorological works in the western
57 Mediterranean area show that extreme storms and cyclones show a complex variability in the
58 sense of non-uniform spatial and temporal patterns (Trigo et al., 2000; Lionello et al., 2006;
59 Gaertner et al., 2007). This is in partly due to the lack of a clear large scale pattern which may be
60 expected when dealing with intense events, as the number of events is low with irregular intensity
61 and intervals. More long-term observations or palaeo-reconstructions in different areas of the
62 western Mediterranean are needed. Tsunamis are known to occur in the Mediterranean Sea where
63 all types of sources earthquakes, volcanic eruptions and landslides from the continental margins
64 are active. There are evidences of large tsunamis during the historical and pre-historical period,
65 especially in the tectonically more active eastern Mediterranean (e.g., Kelletat and Schellmann,

66 2002; Morhange et al., 2006). The western part of the basin has also been reported as tsunami-
67 exposed. Historic events have been reported from the Algerian coast and tsunami propagation has
68 been modelled (Alvarez-Gomez et al., 2011). Geomorphic evidence of ancient tsunami impacts
69 has also been documented (Maouche et al., 2009). A long-term record of tsunami and storm
70 activity on time scales of centuries to millennia is especially important in understanding the
71 temporal variability of these extreme events.

72

73 This study focuses mainly on the Murcia province in Spain (Figure 1). This lowland
74 Mediterranean coast is sensitive to risks of submersion during extreme events. We propose to use
75 a high-resolution geochemical and sedimentological approach to reconstruct past surge events in
76 the Mar Menor lagoon, and then confront our results with extreme historical coastal events in the
77 western Mediterranean.

78

79 2. Study site

80

81 The Mar Menor lagoon is the largest lagoon on the Spanish Mediterranean coast, located at the
82 SE of the Iberian Peninsula, in the region of Murcia in the area called Campo de Cartagena basin
83 (Lat. 37.786129, Lon. 0.810450, Figure 1). This coastal lagoon occupies an area of
84 approximately 135 km² with an average depth of 3.6 m. This lagoon is separated from the
85 Mediterranean sea by La Manga, which is a sandy barrier of 20 km long, between 30 and 500 m
86 wide and less than 3 m above sea level. This sandy barrier is crossed by five, more or less
87 functional, channels or “golas”. The Campo de Cartagena Basin represent 1,440 km², with an
88 elevations ranging from the sea level to 1065 m, surrounded by the Mediterranean Sea to the

89 East, the anticline of Torrevieja to the North and the Cartagena-La Unión mountain range to the
90 south. This basin is filled by sediments from early Miocene to Quaternary. The major lithologies
91 are composed of sand, silt, clay conglomerate, caliche and sandstone of the Quaternary period;
92 marl, conglomerate and gypsum for the Miocene and Pliocene periods (Jiménez-Martínez et al.,
93 2012). The lagoon and the northern salt marshes of San Pedro are protected for their ecological
94 importance (Special Protected Area of Mediterranean Interest, Natura 2000 network and
95 Ramsar). The area is impacted by residual past mining activity, agricultural activities (intensive
96 fruits and vegetable production), and urban growth coupled with touristic development since
97 1956 (Pérez-Ruzafa et al., 1987; 1991; 2005). Most of La Manga area is urbanized, a population
98 of 10,000 inhabitants live here all year long, and growing to ~ 200,000 habitants during summer.
99 High population density and low level topography makes the area very sensitive to the impact of
100 climate change and sea level rise. Mar Menor lagoon is considered as one of the Spanish coast
101 most threatened site by the mean sea level rise and possible increase of extreme climatic events.

102

103

104 3. Materials and methods

105

106 3.1 Core material

107

108 A 4-m-long piston core (MM2) was collected in the Mar Menor lagoon in September 2011
109 (Figure 1) with the UWITEC[®] gravity coring platform (Laboratoire des Sciences du Climat et de
110 l'Environnement and University of Chambéry) using a simplified piston corer of 2 m length and
111 83 mm inner diameter. Two consecutive sections (0 to 2 m and 2 to 4m sediment depth,

112 respectively, were cored from a first position followed by a third section (1 to 3m) from a
113 position ca 1 m apart to cover the technical hiatus between the first two sections. MM2 core was
114 collected at 4 m below sea level.

115

116 3.2 Physical measures

117

118 Back to the laboratory, the structure of the sediment was studied using the Scopix X-ray scanning
119 (EPOC, University of Bordeaux 1) and photographed. This was complemented by granulometric
120 analyses on contiguous 1-cm samples using a Beckman-Coulter LS13320 laser diffraction
121 particle-size analyser (Géosciences Montpellier). XRF analysis were performed on the surface of
122 split sediment core MM2 every 0.5 cm using a non-destructive Avaatech core-scanner (EPOC,
123 Université Bordeaux 1). The split core was covered with a 4 μm thin Ultralene to avoid
124 contamination. Geochemical data was obtained at different tube voltage, 10 kV for Al, Si, S, Cl,
125 K, Ca, Ti, Mn, Fe and 30 kV for Zn, Br, Sr, Rb, Zr (Richter et al., 2006).

126

127

128 3.3 Macro-fauna

129

130 To study mollusc shells, samples were taken every 2 cm and sieved at 1mm. Macro-fauna
131 samples were taken at fixed volume (100 cm^3). Individuals were determined to the lower
132 taxonomic level possible (species or genera) and counted. Assemblage structure was estimated by
133 mean of species richness (S), taxon abundance (n_i) and total abundance (N).

134

135 3.4 Geochronology

136
137 The chronology of core MM2 was carried out using ^{137}Cs and ^{210}Pb method on a centennial time-
138 scale by gamma spectrometry at the Géosciences Montpellier Laboratory (Montpellier, France).
139 ^{14}C analyses were realized on mollusk shells at the Laboratoire de Mesure on ARTEMIS in CEA
140 institute at Saclay. These measurements were obtained from monospecific samples of
141 *Cerastoderma glaucum* at each level. ^{14}C ages were corrected for reservoir age (see Sabatier et
142 al., 2010 for method) and converted to calendar years using the computer program OxCal v4.2
143 (Bronk Ramsey, 2001, 2008) at two standard deviations (see chapter 4.3).

144

145 3.5 Spectral analyses

146 Cyclic patterns in the Mar Menor lagoonal sequence were studied from spectral analyses by using
147 two methods in order to reduce possible biases of a single method (Desprat et al., 2003). We used
148 the maximum entropy method (MEM) and the multi-taper method (MTM). The MEM selects the
149 spectrum with the highest entropy, which represents the least biased estimate for the given
150 information, or put in other terms, the maximally noncommittal with regard to missing
151 information (Harremoës and Topsoe, 2001). The spectrum obtained by this method shows an
152 excellent frequency resolution with sharp spectral features (Berger et al., 1991; Dubar, 2006;
153 Pardo-Iguzquiza and Rodriguez-Tovar, 2006). The MTM is a non-parametric method that (1)
154 reduces the variance of spectral estimates by combining multiple orthogonal windows in the time
155 domain before Fourier transforming, and (2) provides a narrowband F-test useful to assess the
156 significance of periodic components (Thomson, 1982, 1990; Percival and Walden, 1993).

157

158

159 4. Results

160

161 4.1 Core description

162

163 Photo, X-ray images, X-ray fluorescence and high-resolution grain-size analysis for MM2
164 indicate several thin, coarse-grained layers preserved within mud sediments. These coarse layers
165 are constituted by a mixture of shell debris and siliciclastic sand and have basal boundaries easily
166 identified from a change to coarser grain size and darker colour on X-ray images (Figure 2a).
167 These coarser grain size layers indicate “energetic” events, relative to the background
168 sedimentation (i.e mud facies) and are probably link to washover events (storm or tsunami).

169

170 4.2 Sediment source

171 The terrigenous fraction in Mar Menor lagoon is mainly controlled by terrestrial and marine
172 inputs. The core (MM2) was collected at 800 m from the sandy barrier and more than 8,500 m
173 from the different river mouths. On our study site, watercourses are the source of fine fraction
174 dispersed in the lagoon and marine inputs are characterized by coarse sands. The lagoon barrier
175 beach sand samples show unimodal distribution with a mean grain population ranging between
176 160 and 653 μm . The percentages of this grain population decrease from the sea to the lagoon in
177 surface samples (Figure 2b). The evolution with depth of this population displays eight main
178 changes in MM2 core revealed by the grey bands on Figure 3. The main peaks of coarse sands
179 occur around 290, 255, 210, 170, 150, 60, 40 and 5 cm (Figure 3).

180 Major chemical elements using the ITRAX core scanner provide high-resolution
181 palaeoenvironmental information in a variety of sedimentary environments. In the present study
182 we chose the ratio Si/Al and Zr/Al that better discriminate between the two source areas, marine
183 vs drainage basin (Dezileau et al., 2011, Sabatier et al., 2012; Raji et al., 2015). The high Zr/Al
184 ratio value is probably explained by the presence of heavy minerals (like zircon) from marine
185 sand and the high Si/Al ratio is due to Quartz minerals in marine sand. Si/Al and Zr/Al ratios
186 have the same evolution with depth, especially in the first three meters of the sediment core
187 (Figure 4, shaded bands).

188 A fundamental step in the core analysis is to establish criteria to correctly identify overwash
189 layers. We systematically used grain size variation and geochemical signatures (i.e. Si/Al and
190 Zr/Al ratios). As the background sedimentation shows a fine silt facies, we consider values higher
191 than 20% of the 63 μ m fraction as outlining “high energy” events (Figure 3). Positive anomalies
192 of the Si/Al and Zr/Al ratios above 12 and 2.5 respectively (Figure 4), indicate a higher relative
193 contribution of marine sand. The marine origin of these “high energy” events was also
194 highlighting through molluscs identification (*Bittium reticulatum* and *Rissoa ventricosa*) (see
195 chapter 4.3, Figure 6).

196

197 4.3. Faunal variations

198

199 Macro-fauna analyses are a good indicator of a lagoon palaeo-isolation state. While total
200 abundance and relative abundance of individuals of the different species is a good indicator of
201 environmental stress and lagoon productivity, species richness is a good indicator of marine
202 influence because species develop in different ranges of salinity, temperature and oxygenation

203 and colonization of marine species into the lagoon environments depends of the isolation degree
204 and connectivity between both systems (Pérez-Ruzafa and Marcos, 1992; Pérez-Ruzafa et al.,
205 2005). Figure 5 shows the variation of the number of species and total abundance (number of
206 individuals in 100 cm³) along the studied time series. Taxon richness ranges between 0, at depths
207 higher than 365 cm, and 18 reached at a 260 cm depth. The impoverished depths, after the earlier
208 azoic one, corresponds to 302-362 cm with a mean of 4.76 taxons, 72-78 cm with a mean of 5
209 taxons and 30-36 cm with a mean of 5.7 taxons. The depths with highest species richness are
210 from 192 to 266 cm and from 81 to 186 cm. These depths would correspond to a higher marine
211 influence. Above 150 cm takes place a progressive impoverishment in the number of species
212 reflecting a progressive isolation of the Mar Menor from the Mediterranean Sea, with punctual
213 peacks in species richness, probably related to episodes of rupture of the sandbar (Figure 5). The
214 total abundance confirm

215 The most frequent species, present in more than 50% of the samples, excluding the azoic depths,
216 are *Corbula gibba* (Olivi, 1792) (92.4%), *Bittium reticulatum* (da Costa, 1778) (84.9%), *Tellina*
217 *sp* (78.9%), *Pusillina* (=Rissoa) *lineolata* (Michaud, 1830) (78.2%), *Acanthocardia*
218 *paucicostata* (G. B. Sowerby II, 1834) (77.3%), *Cerastoderma glaucum* (Bruguière, 1789)
219 (71.4%), *Anthalis sp* (63.9%), *Abra sp* (74.8%), *Loripes lacteus* (Linnaeus, 1758) (61.3%) and
220 *Philine aperta* (Linnaeus, 1767) (59.7%). Hydrobiidae *sp* appear in 47.9 % of the samples, but is
221 restricted to the upper 150 cm, constituting 61.5% of the assemblage at 15 cm depth section. This
222 specie is a typical lagoon inhabitant. *Conus ventricosus* (Gmelin, 1791) appears only in the
223 13.5% of the samples, comprised between 162 and 293 cm depth, reaching dominance up to 7%
224 of the assemblage, but characterizes typical marine conditions, reinforced with the presence of
225 abundant seurchin spines.

226 Data of Figure 6 show a main change in mollusc population at around 150-130 cm characterized
227 by an increase of the most typical lagoonal specie *Hydrobia acuta*, whereas the abundance of
228 species with marine affinity like *Pusillina* (=Rissoa) *lineolata* and *Conus ventricosus* decrease
229 (Figure 6). This main change in mollusc population also reveals a major palaeoenvironmental
230 change around 150 cm, this faunal variation is probably due to a change in environmental context
231 from a lagoonal environment, with a marine influence to a more isolated environment.

232

233 4.4 Age model

234

235 The chronology of core MM2 has been established for the last 6,500 years BP using ^{137}Cs , ^{210}Pb
236 and (AMS) ^{14}C dates on monospecific shell samples, geochemical analysis of mining-
237 contaminated lagoonal sediments and palaeomagnetism (Dezileau et al., in prep). Radiocarbon
238 age of lagoonal and marine organisms is usually older than the atmospheric ^{14}C age and has to be
239 corrected by subtraction of the “reservoir age” (Siani et al., 2001; Reimer and McCormac 2002;
240 Zoppi et al., 2001; Sabatier et al., 2010; Dezileau et al., 2015). We evaluated the modern
241 reservoir ^{14}C age by comparing an age derived from ^{137}Cs , ^{210}Pb data and geochemical analysis of
242 mining-contaminated lagoonal sediments with an AMS ^{14}C age of a pre-bomb mollusc shell (see
243 Sabatier et al., 2010 for method). The reservoir age (R(t)) with a value of 1003 ± 62 ^{14}C yr is 600
244 yr higher than the mean marine reservoir age (around 400 yr) and may be explained by an
245 isolation of the lagoon from the Mediterranean Sea. This high reservoir age value is similar to
246 other estimates in different Mediterranean lagoons (Zoppi et al., 2001; Sabatier et al., 2010).
247 ^{14}C ages were also obtained on a series of Holocene mollusc shells sampled at different depths of
248 the ~2-m-long core MM2 (Figure 7, Dezileau et al., in prep). Comparing palaeomagnetic ages

249 and ^{14}C ages versus depth, we show that the reservoir age has changed in the past and was lower
250 (505 yr) than the modern value (1003 yr, Dezileau et al., in prep). This change was also observed
251 in another Mediterranean lagoons (Sabatier et al., 2010). In the Mar Menor lagoon, Linear
252 Sedimentation Rate (LSR) obtained for the core MM2 suggest a low mean accumulation rate of
253 0.6 mm.yr^{-1} , from the base to the top of the core.

254

255 5. Discussion

256

257 5.1 Site sensitivity to overwash deposits

258

259 Site sensitivity to overwash deposits may result from different factors such as barrier-elevation,
260 sediment supply, inlet, and change in sea level (Donnelly and Webb, 2004; Scileppi and
261 Donnelly, 2007, Dezileau et al., 2011). An increase of sea level induces a shift of the barrier
262 landward. Therefore, an increase of sand layers in a sediment core may be due to a sea level
263 change. In the Mediterranean Sea, the sea level has remained more or less constant during the last
264 5000 yrs ($< 2\text{m}$, Pirazzoli, 1991; Lambeck and Bard, 2000). Before this period, a significant
265 change in sea level occurred. During the first phase of lagoonal sediment deposit (between 6500
266 and 5000 years Cal BP), the number of sand layers is low. The sandy barrier was probably at
267 more than 1 km from the present position and may probably explain why sand layers are not
268 observed. The strong increase in coarse grain layer frequency after ca 5400 years Cal BP can be
269 explained by a migration of the barrier up to a position, which is not far away from the present
270 position.

271 Fauna content reveals a major palaeoenvironmental change around 150 cm (i.e. 2400 yr cal BP,
272 Figure 6). Such change is probably due to a shift from a leaky lagoon to a restricted and choked
273 lagoon environment, sensu Kjerfve (1996). Thus, after this date (i.e 2400 yr cal BP) the barrier
274 was continuous with sometimes inlet formation in relation to intense overwash events. To
275 conclude, between 2400 yr cal BP and today, the lagoon is isolated from the sea. During this
276 period the general morphology of the lagoon and the barrier have not changed drastically.
277 Between 5400 yr cal BP and 2400 yr cal BP the lagoon was less isolated from the Mediterranean
278 Sea, typical from a leaky lagoon environment. During this period, fine sediments were
279 accumulated. The lagoon experienced quiescent sedimentation probably protected behind a sandy
280 barrier more or less continuous. The presence of sand layers may be interpreted by intense
281 overwash events. Between 6500-5400 yrs BP, the morphology of the lagoon and the barrier is
282 different. The position of the sandy barrier was far away from the present position. In that case,
283 the number and the intensity of surge events recorded are not comparable to the upper part of the
284 core (Figures 3 and 8). During this period, the lack of sand layers does not mean no surge events
285 but simply they are not recorded.

286 The record of paleostorm events can be complicated by different factors, however, the clay/silt
287 sediment types appearing throughout the record show that this area was experiencing quiescent
288 sedimentation, indicating that the site was protected behind a sandy barrier over that time.
289 Moreover, in order to control localized sensitivity changes, it will be necessary in the future to
290 employ a multiple-site approach, as extreme storms or tsunamis in all this area would likely result
291 in surges and waves of sufficient height to overtop the barrier across wide stretches of coast and
292 not only in a localized area.

293

294 5. 2 Storms or tsunamis?

295 The Zr/Al and Si/Al ratios of sandy layers are above 12 and 2.5 respectively (Figure 8),
296 indicating a higher relative contribution of marine sand. The marine origin of these “high energy”
297 events was also highlighted through molluscs identification (*Bittium reticulatum* and *Rissoa*
298 *ventricosa*, Figure 8). This multiproxy approach suggests the occurrence of eight periods of
299 increase of overwash events reflecting perturbations of coastal hydrodynamic due to palaeostorm
300 or palaeotsunami events (grey band on Figure 8).

301 Both tsunamis and storms induce coastal flooding. It is difficult to discriminate storm and
302 tsunami deposits (Kortekaas and Dawson, 2007; Morton et al., 2007; Engel and Brückner, 2011).

303 The coarse-grained layers observed in the core MM2 could be a signature of tsunamis or storms.
304 Records of historic and contemporary coastal hazards (storms and tsunamis) may help us to
305 determine which historical events left a sedimentological signature in the Mar Menor lagoon.

306 In textual archives, extreme storm events were described due to the strong economic and societal
307 impact of these events (Seisedos et al., 2013). For the last 200 years, 27 storms affected the
308 coast of Murcia. Among all of these storms, some seems to be more catastrophic. The storm of
309 November first, 1869 produced the wreckage of a numerous ships in the Torrevieja harbour.

310 Between Isla Grosa and San Pedro del Pinatar more than thirty-five ships sank and crashed. In
311 the Mar Menor lagoon, fifty fishing boats were destroyed and thrown to the ground. Wave
312 heights associated with this storm were estimated higher than 8 m off the La Manga sandbar.

313 This severe storm also affected La Union and Cartagena cities destroying houses and paralyzing
314 it for many days. From the hydrological and ecological point of view, the 1869 storm led to
315 drastic and persistent changes in the salinity of the lagoon and to the colonization of new species
316 of marine origin (Navarro, 1927), affecting also the fisheries in the lagoon (Pérez-Ruzafa et al.,

317 1991). There are historical references to some other storms that led to the breaking of the sandbar
318 in the Mar Menor (in 1526, 1676, 1687, 1690, 1692, 1694, 1706, 1762, 1765, 1787, 1795)
319 (Jiménez de Gregorio, 1957; Pérez-Ruzafa et al., 1987), although there is no information about
320 their magnitude, the extent and exact location of the breaks and their impact on the lagoon
321 environment. Some ups and downs in the number of species observed in Figure 5 could be
322 related to these events, but an extensive and detailed study would be required for understanding
323 the relationship between the frequency, duration and intensity of the storms and the spatial and
324 temporal scales of their effects and their impact on the fossil record.

325 Different tsunamis occurred on the Spanish coasts, they are more catastrophic and intense on the
326 Atlantic than on the Mediterranean side (Alvarez-Gomez et al., 2011). In the occidental part of
327 the Mediterranean area, there are historical disastrous tsunami events recorded. In Northern
328 Algeria, in addition to the 2003 tsunami, the first well documented event remains the tsunami in
329 the Djijelli Area associated with the seismic event of August 1856, which was also recorded in
330 the Balearic Islands (Maouche et al., 2009). In the Alboran Sea area some reports mention
331 tsunamis that affected the African and Spanish coasts in 1790, 1804 and 1522 (IGN, 2009). For
332 an earthquake magnitude 6.8 (2003 Boumerdes earthquake) with its epicenter calculated at 15 km
333 offshore of Zemmouri, Wang and Liu (2005) show a regional character of the tsunami
334 phenomenon from a numerical simulation. The tsunami propagating from the Algerian coast to
335 the Murcia Province has a lesser amplitude and the tsunami wave height is low (< 25 cm). The
336 Boumerdes-Zemmouri tsunami did not induce any damage along the province of Murcia and the
337 La Manga sandbar. Alvarez-Gomez et al. (2011) identified the hazardous sources and the areas
338 where the impact of tsunamis is greater from numerical simulations. From a set of 22 seismic
339 tsunamigenic sources, the Maximum Wave Elevation was estimated between 0.5 and 1 m along

340 the South-Eastern Spanish coast. All these historical events have been classified as a magnitude
341 between 1 and 3 in the Tsunami Intensity Scale (on a scale of 6 for a maximum intensity,
342 Maramai et al., 2014). Since these different historical events have a magnitude equal or lower
343 than the Boumerdes-Zemmouri tsunami (3 in the Tsunami Intensity Scale), and that this event did
344 not affect significantly La Manga sandbar and the Province of Murcia, considering the available
345 data, historical tsunami events do not seem to be associated to the different sand layers in the
346 Mar Menor lagoon for the last 500 years. From the “Catálogo de Tsunamis en las Costas
347 Españolas”, no tsunamis are recorded along the South Eastern coast of Spain from -218 BC to
348 1756 AD. No information on the existence of tsunamis is recorded over longer periods of time.
349 However, more than 100 boulders were identified along the coastal zone of Algiers and Maouche
350 et al. (2009) suggested that the deposition of the biggest boulders could be attributed to tsunami
351 events. The radiocarbon results highlight two groups of boulders dated to around 419 AD and
352 1700 AD. Although no historical accounts report these events, tsunami events are extremely rare
353 and mainly of low magnitude and cannot be at the origin of the different sand layers in the Mar
354 Menor lagoon.

355 To determine which historical events may let sandy layers, we compared our high-resolution
356 record of past extreme sea events from the core MM2 to the catalogue of historical storm and
357 tsunami events in the area. The first coarse-grained event layer has been dated at 80 cal. BP (i.e.
358 1880 A.D+/-30 years). This sandy deposit could be associated to the storm of November first,
359 1869, recorded in many city archives between Cartagena and Torrevieja and in the Mar Menor,
360 and considered as the most catastrophic storm event in the Province of Murcia for the last 200
361 years. In the core MM2, no sand layers are consistent with the Algerian tsunamis dated to around
362 419 AD and 1700 AD (Figure 8). There is evidence that this sand layer is compatible with large

363 storm waves.

364

365 5.3 Storm activity in the context of past climatic changes

366

367 Based on our ^{14}C age model, marine coarse grained event layers occurred around 5250, 4000,
368 3600, 3010, 2300, 1350, 650 and 80 years cal BP. Except one period dated at 3600 years cal BP,
369 the seven other periods of most frequent surge events in the Mar Menor lagoon seem to coincide
370 with the coldest periods in Europe during the late Holocene, taking into account chronological
371 uncertainty (Figure 8, Bond et al., 2001). A spectral analysis was performed on the ca 6.5-kyr
372 time series of the sand percentage from the MM2 sequence. The results show four major
373 frequencies with high spectral power densities and significant F-test values at ca 8×10^{-4} , 1.4×10^{-3} ,
374 1.8×10^{-3} , and $3.1 \times 10^{-3} \text{ yr}^{-1}$ (Figure 9A). Considering the full width at half maximum (FWHM) of
375 these peaks on the MTM spectrum, this yields respective periodicities of 1228 ± 327 , 732 ± 80 ,
376 562 ± 58 , and $319 \pm 16 \text{ yr}$ for the MM2 sand % proxy. Multi-centennial to millennial timescale
377 climate variabilities similar to these periodicities have been reported in the literature for the
378 Holocene (Bond et al., 1997, 2001; Langdon et al., 2003; Debret et al., 2007, 2009; Wanner et al.,
379 2011; Kravchinsky et al., 2013; Soon et al., 2014). Amongst the well-known proxies that have
380 revealed a millennial-scale climate variability during the Holocene, the ice-rafted debris (IRD)
381 indices in North Atlantic developed by Bond et al. (1997, 2001) present a cyclicity of 1470 ± 500
382 yr, which matches the $1228 \pm 327 \text{ yr}$ periodicity evidenced in the Mar Menor lagoon, considering
383 the respective uncertainties on the periodicities. When filtering the raw data of the Mar Menor
384 sand % record by a Gaussian filter with a frequency of $8 \times 10^{-4} \text{ yr}^{-1}$ (1228 years), six cycles appear
385 with a noteworthy enhancement of the cyclic amplitude after 5500 cal yr BP (Figure 9B). The
386 five ascending phases occurring on the 1228-yr filtered curve at ca 5715/5115, 4525/3945,

387 3365/2775, 2145/1215, and 575/-35 cal yr BP approximate the high storm activity periods
388 evidenced in the French Mediterranean lagoon of Pierre-Blanche for the last 7000 years (Sabatier
389 et al., 2012).

390 The origin of the storminess periods evidenced by the spectral analysis in the Mar Menor lagoon
391 can be discussed in the light of previous works mentioning analogous climate variabilities during
392 the Holocene. Bond et al. (1997, 2001) associated the 1470 ± 500 yr IRD cycle to a solar forcing,
393 amplified by a change of North Atlantic Deep Water production. Langdon et al. (2003) found a
394 sub-millennial climate oscillation in Scotland possibly related to the North Atlantic thermohaline
395 circulation (THC). Moreover, Debret et al. (2007, 2009) showed a cyclicity of 1500 yr since the
396 Mid-Holocene probably link to an internal forcing due to the THC.

397 Concerning the multi-centennial periodicities, Soon et al. (2014) used global proxies to evidence
398 a 500-yr fundamental solar mode and to identify intermediate derived cycles at 700 and 300-yr
399 which could be rectified responses of the Atlantic THC to external solar modulation and pacing.

400 Kravchinsky et al. (2013) found also a 500-yr climate cycle in the southern Siberia presumed to
401 be derived by increased solar insolation and possibly amplified by other mechanisms. Some
402 authors found a relationship between the ca 700-yr period and the monsoonal/ITCZ regimes in
403 equatorial Africa (Russell et al., 2003; Russell and Johnson, 2005), southern Asian (Staubwasser
404 et al., 2003), and eastern Arabian Sea (Sarkar et al., 2000), while other authors suggested that the
405 ca 700-800 yr period could be a subharmonic mode derived from the fundamental 1500-year
406 cycle of the THC (Von Rad et al., 1999; Wang et al., 1999). Besides, Rimbu et al. (2004)
407 mentioned a 700 yr variability from sea-surface temperature (SST) records in the tropical and
408 North Atlantic. Hence, our results seem to indicate that the Late Holocene multi-centennial
409 variability of the cyclogenesis in Western Mediterranean was steered by both, external (solar) and
410 internal (THC/ITCZ) forcings. Further investigations of additional sequences and high-resolution

411 coastal imagery will be required to assert reliably the origin of these multi-centennial periods in
412 the Mediterranean area.

413

414 7. Conclusion

415 This study provides a 6500-yr high-resolution record of past overwash events using a multi-proxy
416 approach of a sediment core from the Mar Menor lagoon in Spain in the Western Mediterranean
417 Sea. Eight sandy layers are preserved in the core and seems to be associated to periods of
418 increased extreme sea events. The results indicate little likelihood of a tsunami origin for these
419 coarse grained layers, although historical tsunami events are recorded in this area. These surge
420 events seem to coincide with climatic cold periods in Europe during the late Holocene,
421 suggesting a control by a climatic mechanism for periods of increased storm activity. From the
422 available data, we have identified seven periods of high storm activity at around 5250, 4000,
423 3600, 3010, 2300, 1350, 650 and 80 years cal BP. Except one period dated at 3600 years cal BP,
424 the seven other periods of most frequent surge events in the Mar Menor lagoon seem to coincide
425 with the coldest periods in Europe during the late Holocene, taking into account chronological
426 uncertainty. Spectral analyses performed on the sand % revealed four major periodicities of 1228
427 ± 327 , 732 ± 80 , 562 ± 58 , and 319 ± 16 yr. The origin of the storminess periods evidenced by the
428 spectral analysis in the Mar Menor lagoon can be discussed in the light of previous works
429 mentioning analogous climate variabilities during the Holocene. Our results seem to indicate that
430 the Late Holocene multi-centennial variability of the cyclogenesis in Western Mediterranean was
431 steered by both, external (solar) and internal (THC/ITCZ) forcings. However, further
432 investigations, such as additional coring, high-resolution coastal imagery, are needed to better
433 constrain the main cause of these multiple-events.

434

435

436 Acknowledgments

437

438 The authors would like to thank all participants in the coring expedition, particularly E. Regnier
439 (Technician, LSCE - IPSL, Paris) for his collaboration in the various stages of this study. This
440 study is funded by the MISTRALS PALEOMEX project. We thank the Laboratoire de Mesure
441 ^{14}C (LMC14) ARTEMIS in the CEA Institute at Saclay (French Atomic Energy Commission) for
442 the ^{14}C analyses. This article benefited through constructive reviews by Stella Kortekaas and
443 Suzanne Leroy.

444

445

446 References

447

448 Álvarez-Gómez, J. A., González, M., and Otero, L.: Tsunami hazard at the Western
449 Mediterranean Spanish coast from seismic sources, *Natural Hazards and Earth System*
450 *Science*, 11, 227-240, 2011.

451 Berger, A., Melice, J.-L., Hinnov, L.: A strategy for frequency spectra of Quaternary climate
452 records. *Climate Dynamics* 5, 227-240, 1991.

453 Bond, G., Kromer, B., Beer, J., Muscheler, R., Evans, M. N., Showers, W., Hoffmann, S., Lotti-
454 Bond, R., Hajdas, I., and Bonani, G.: Persistent solar influence on North Atlantic climate
455 during the Holocene, *Science*, 294, 2130-2136, 2001.

456 Bond, G., Showers, W., Cheseby, M., Lotti, R., Almasi, P., DeMenocal, P., Priore, P., Cullen, H.,
457 Hajdas, I., Bonani, G.: A pervasive millennial-scale cycle in North Atlantic Holocene and
458 Glacial climates. *Science* 278, 1257-1266, 1997.

459 Bronk Ramsey, C., Development of the Radiocarbon calibration program OxCal, *Radiocarbon*,
460 43, 355-363, Proceedings of 17th International 14C Conference, 2001.

461 Bronk Ramsey, C., Deposition models for chronological records, *Quaternary Science reviews*,
462 27, 42-60, 2008.

463 Debret, M., Bout-Roumazielles, V., Grousset, F., Desmet, M., McManus, J.F., Massei, N., Sebag,
464 D., Petit, J.-R., Copard, Y., Trentesaux, A.: The origin of the 1500-year climate cycles in
465 Holocene North-Atlantic records. *Climate of the Past* 3, 569-575, 2007.

466 Debret, M., Sebag, D., Crosta, X., Massei, N., Petit, J.-R., Chapron, E., Bout-Roumazielles, V.:
467 Evidence from wavelet analysis for a mid-Holocene transition in global climate forcing.
468 *Quaternary Science Reviews* 28, 2675-2688, 2009.

469 Desprat, S., Sanchez-Goni, M.F., Loutre, M.-F.: Revealing climatic variability of the last three
470 millennia in northwestern Iberia using pollen influx data. *Earth and Planetary Science*
471 *Letters* 213, 63-78, 2003.

472 Dezileau, L., Pérez-Ruzafa, A., Camps P., Blanchemanche P., Grafenstein U., Holocene
473 variations of radiocarbon reservoir ages in the Mar Menor lagoon system, *Radiocarbon*, in
474 prep.

475 Dezileau, L., Sabatier, P., Blanchemanche, P., Joly, B., Swingedouw, D., Cassou, C., Castaings,
476 J., Martinez, P., and Von Grafenstein, U.: Intense storm activity during the Little Ice Age
477 on the French Mediterranean coast, *Palaeogeography, Palaeoclimatology, Palaeoecology*,
478 299, 289-297, 2011.

479 Dezileau L., Lehu R., Lallemand S., Hsu S-K., Babonneau N., Ratzov G., Lin A.T., Dominguez
480 S., Historical reconstruction of submarine earthquakes using ²¹⁰Pb, ¹³⁷Cs and ²⁴¹Am
481 turbidite chronology and radiocarbon reservoir age estimation off East Taiwan.
482 Radiocarbon. doi:10.1017/RDC.2015.3, 2016.

483 Donnelly, J. P., Webb III, T., Murnane, R., and Liu, K.: Backbarrier sedimentary records of
484 intense hurricane landfalls in the northeastern United States, Hurricanes and Typhoons:
485 Past, Present, and Future, 58-95, 2004.

486 Dubar, M.: Approche climatique de la période romaine dans l'est du Var : recherche et analyse
487 des composantes périodiques sur un concrétionnement centennal (Ier-IIe siècle apr. J.-C.)
488 de l'aqueduc de Fréjus. ArchéoSciences 30, 163-171, 2006.

489 Engel, M., and Brückner, H.: The identification of palaeo-tsunami deposits—a major challenge in
490 coastal sedimentary research, Dynamische Küsten—Grundlagen, Zusammenhänge und
491 Auswirkungen im Spiegel angewandter Küstenforschung. Proceedings of the 28th Annual
492 Meeting of the German Working Group on Geography of Oceans and Coasts, 2011, 22-25,

493 Gaertner, M.A., Jacob, D., Gil, V., Domínguez, M., Padorno, E., Sánchez, E., Castro, M. :
494 Tropical cyclones over the Mediterranean Sea in climate change simulations. Geophysical
495 Research Letters 34. doi:10.1029/2007GL029977, 1-5, 2007.

496 Harremoës, P., Topsoe, F.: Maximum entropy fundamentals. Entropy 3, 191-226, 2001.

497 IGN: Catalogo de Tsunamis en las Costas Espanolas. Instituto Geografico Nacional, www.ign.es,
498 2009.

499 Jimenez de Gregorio, F.: *El Municipio de San Javier en la historia del Mar Menor y su ribera.*
500 Ayuntamiento de San Javier, Murcia, 1957.

501 Kelletat, D., and Schellmann, G.: Tsunamis on Cyprus: field evidences and 14C dating results,
502 Zeitschrift für Geomorphologie, NF, 19-34, 2002.

503 Kjerfve, B.: Coastal lagoons. In Kjerfve B (ed). *Coastal lagoon processes*. Elsevier
504 Oceanography Series 60: 1-8, 1994.

505 Kortekaas, S., and Dawson, A.: Distinguishing tsunami and storm deposits: an example from
506 Martinhal, SW Portugal, *Sedimentary Geology*, 200, 208-221, 2007.

507 Kravchinsky, V.A., Langereis, C.G., Walker, S.D., Dlusskiy, K.G., White, D.: Discovery of
508 Holocene millennial climate cycles in the Asian continental interior: Has the sun been
509 governing the continental climate? *Global and Planetary Change* 110, 386-396, 2013.

510 Lambeck, K., and Bard, E.: Sea-level change along the French Mediterranean coast for the past
511 30 000 years, *Earth and Planetary Science Letters*, 175, 203-222, 2000.

512 Langdon, P.G., Barber, K.E., Hugues, P.D.M.: A 7500-year peat-based palaeoclimatic
513 reconstruction and evidence for an 1100-year cyclicity in bog surface wetness from Temple
514 Hill Moss, Pentland Hills, southeast Scotland. *Quaternary Science Reviews* 22, 259-274,
515 2003.

516 Lionello, P., Bhend, J., Buzzi, A., Della-Marta, P.M., Krichak, S., Jansá, A., Maheras, P., Sanna,
517 A., Trigo, I.F., Trigo, R. : Cyclones in the Mediterranean region: climatology and effects on
518 the environment, in *Mediterranean Climate Variability*. In: Lionello, P., Malanotte-Rizzoli,
519 P., Boscolo, R. (Eds.), *Mediterranean Climate Variability*. : *Developments in Earth and*
520 *Environmental Sciences*, 4. Elseviered., 324–372, 2006.

521 Maouche, S., Morhange, C., and Meghraoui, M.: Large boulder accumulation on the Algerian
522 coast evidence tsunami events in the western Mediterranean, *Marine Geology*, 262, 96-104,
523 2009.

524 Maramai, A., Brizuela, B., and Graziani, L.: The Euro-Mediterranean Tsunami Catalogue,
525 *Annals of Geophysics*, 57, S0435, 2014.

526 Morhange, C., Marriner, N., and Pirazzoli, P. A.: Evidence of Late-Holocene Tsunami Events in
527 Lebanon Z. Geomorphol NFSuppl.-Bd., 146, 81-95, 2006.

528 Morton, R. A., Gelfenbaum, G., and Jaffe, B. E.: Physical criteria for distinguishing sandy
529 tsunami and storm deposits using modern examples, *Sedimentary Geology*, 200, 184-207,
530 2007.

531 Navarro, F.: Observaciones sobre el Mar Menor (Murcia). Notas y resúmenes del Instituto
532 Español de Oceanografía, Ser. II, 16:1-63, 1927.

533 Paillard, D., Labeyrie, L., Yiou, P.: Macintosh program performs time-series analysis. *EOS*
534 *Transactions AGU* 77(39), 379-379, 1996.

535 Pardo-Iguzquiza, E., Rodriguez-Tovar, F.J.: Maximum entropy spectral analysis of climatic time
536 series revisited: Assessing the statistical significance of estimated spectral peaks. *Journal of*
537 *Geophysical Research* 111, D10102, 2006.

538 Percival, D.B., Walden, A.T.: *Spectral analysis for physical applications: multitaper and*
539 *conventional univariate techniques*. Cambridge University Press, New York, 583 p, 1993.

540 Pérez-Ruzafa, A., Marcos, C., Pérez-Ruzafa, I., and Ros, J.: Evolución de las características
541 ambientales y de los poblamientos del Mar Menor (Murcia, SE de España), *Anales de*
542 *Biología*, 1987, 53-65,

543 Pérez-Ruzafa, A., Marcos-Diego, C., and Ros, J.: Environmental and biological changes related
544 to recent human activities in the Mar Menor (SE of Spain), *Marine Pollution Bulletin*, 23,
545 747-751, 1991.

546 Pérez-Ruzafa, A., Marcos-Diego, C.: Colonization rates and dispersal as essential parameters in
547 the confinement theory to explain the structure and horizontal zonation of lagoon benthic
548 assemblages. *Rapp. Comm. int. Mer Médit.* 33: 100, 1992.

549

550 Pérez-Ruzafa, A., Marcos, C., and Gilabert, J.: The ecology of the Mar Menor coastal lagoon: a
551 fast-changing ecosystem under human pressure, *Coastal Lagoons*. CRC Press, Boca Racon,
552 392-421, 2005.

553 Pirazzoli, P. A.: World atlas of Holocene sea-level changes, *Elsevier Oceanography Series*, 58, 1-
554 280, 1991.

555 Raji, O., Dezileau L., Snoussi M., and Niazi, S.: Extreme sea events during the last millennium in
556 North-East of Morocco. *Natural Hazards and Earth System Sciences*, 15,203-211, 2015.

557 Reimer P.J., McCormac F.G.: Marine radiocarbon reservoir corrections for the Mediterranean
558 and Aegean seas. *Radiocarbon* 44(1):159–66, 2002.

559 Rimbu, N., Lohmann, G., Lorenz, S.J., Kim, J.H., Schneider, R.R.: Holocene climate variability
560 as derived from alkenone sea surface temperature and coupled ocean-atmosphere model
561 experiments. *Climate Dynamics* 23, 215-227, 2004.

562 Russell, J.M., Johnson, T.C.: Late Holocene climate change in the North Atlantic and equatorial
563 Africa: Millennial-scale ITCZ migration. *Geophysical Research Letters* 32, L17705, 2005.

564 Russell, J.M., Johnson, T.C., Talbot, M.R.: A 725 yr cycle in the climate of central Africa during
565 the late Holocene. *Geology* 31(8), 677-680, 2003.

566 Sabatier, P., Dezileau, L., Blanchemanche, P., Siani, J., Condomines, M., Bentaleb, I., Piques, G.:
567 Holocene variations of radiocarbon reservoir ages in a Mediterranean lagoonal system.
568 *Radiocarbon*, 52, (1), 91-102, 2010.

569 Sabatier, P., Dezileau, L., Colin, C., Briquieu, L., Bouchette, F., Martinez, P., Siani, G., Raynal,
570 O., Von Grafenstein, U.: 7000 years of paleostorm activity in the NW Mediterranean Sea in
571 response to Holocene climate events. *Quaternary Research* 2012, 1-11, 2012.

572 Sarkar, A., Ramesh, R., Somayajulu, B.L.K., Agnihotri, R., Jull, A.J.T., Burr, G.S.: High
573 resolution Holocene monsoon record from the eastern Arabian Sea. *Earth and Planetary*
574 *Science Letters* 177, 209-218, 2000.

575 Scileppi, E., Donnelly, J.P. : Sedimentary evidence of hurricane strikes in western Long Island,
576 NY. *Geochemistry, Geophysics and Geosystems* 8, Q06011. doi:10.1029/ 2006GC001463,
577 2007.

578 Seisdedos, J., Mulas, J., González de Vallejo, L. I., Rodríguez Franco, J. A., Gracia, F. J., Del
579 Río, L., y Garrote, J. :Estudio y cartografía de los peligros naturales costeros de la región
580 de Murcia. *Boletín Geológico y Minero*, 124 (3): 505-520, 2013.

581 Siani G., Paterne M., Michel E., Sulpizio R., Sbrana A., Arnold M., Haddad G. : Mediterranean
582 sea surface radiocarbon age changes since the last glacial maximum. *Science*
583 294(5548):1917–20, 2001.

584 Soon, W., Velasco Herrera, V.M., Selvaraj, K., Traversi, R., Usoskin, I., Arthur Chen, C.-T.,
585 Lou, J.-Y., Kao, S.-J., Carter, R.M., Pipin, V., Severi, M., Becagli, S.: A review of
586 Holocene solar-linked climatic variation on centennial to millennial timescales: Physical
587 processes, interpretative frameworks and a new multiple cross-wavelet transform
588 algorithm. *Earth-Science Reviews* 134, 1-15, 2014.

589 Staubwasser, M., Sirocko, F., Grootes, P.M., Segl, M.: Climate change at the 4.2 ka BP
590 termination of the Indus valley civilization and Holocene south Asian monsoon variability.
591 *Geophysical Research Letters* 30(8), 1425, 2003.

592 Thomson, D.J.: Spectrum estimation and harmonic analysis. *Proceedings of the IEEE* 70(9),
593 1055-1096, 1982.

594 Thomson, D.J.: Time series analysis of Holocene climate data. *Philosophical Transactions of the*
595 *Royal Society of London, Series A, Mathematical and Physical Sciences* 330, 601-616,
596 1990.

597 Trigo, I.F., Davies, T.D., Bigg, G.R., : Decline in Mediterranean rainfall caused by weakening of
598 Mediterranean cyclones. *Geophysical Research Letters* 27, 2913–2916, 2000.

599 Von Rad, U., Schaaf, M., Michels, K.H., Schulz, H., Berger, W.H., Sirocko, F. A 5000-yr Record
600 of Climate Change in Varved Sediments from the Oxygen Minimum Zone off Pakistan,
601 Northeastern Arabian Sea. *Quaternary Research* 51, 39-53, 1999.

602 Wang, L., Sarnthein, M., Erlenkeuser, H., Grimalt, J., Grootes, P., Heilig, S., Ivanova, E.,
603 Kienast, M., Pelejero, C., Pflaumann, U.: East Asian monsoon climate during the Late
604 Pleistocene: high-resolution sediment records from the South China Sea. *Marine Geology*
605 156, 245-284, 1999.

606 Wang, X., Liu, P.L.-F., : A numerical investigation of Boumerdes-Zemmouri (Algeria)
607 earthquake and tsunami. *Computer Modeling in Engineering Science* 10 (2), 171–184,
608 2005.

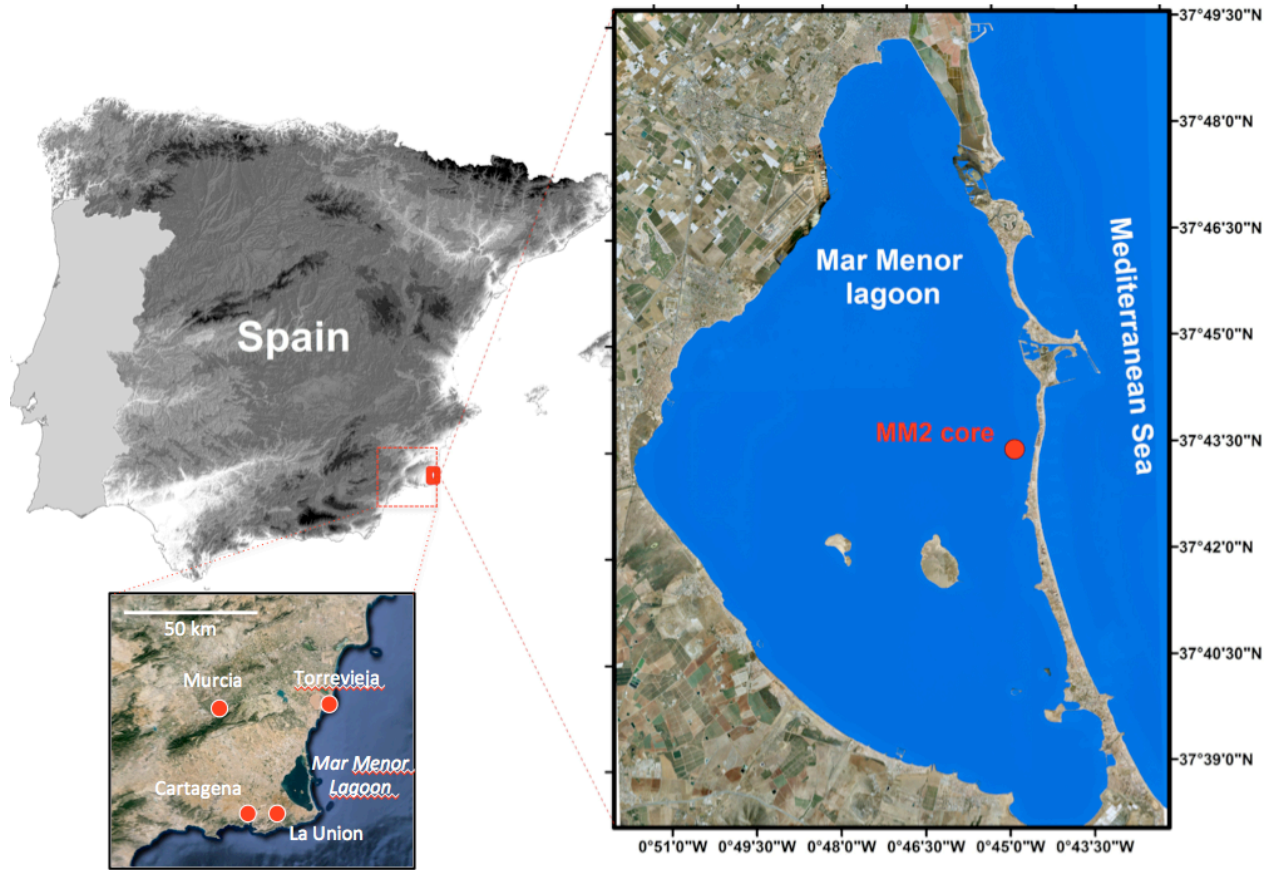
609 Wanner, H., Solomina, O., Grosjean, M., Ritz, S.P., Jetel, M.: Structure and origin of Holocene
610 cold events. *Quaternary Science Reviews* 30, 3109-3123, 2011.

611 Zoppi U., Albani A., Ammerman A.J., Hua Q., Lawson E.M., Serandrei Barbero R. :Preliminary
612 estimate of the reservoir age in the Lagoon of Venice. *Radiocarbon* 43(2A):489–94, 2001.

613

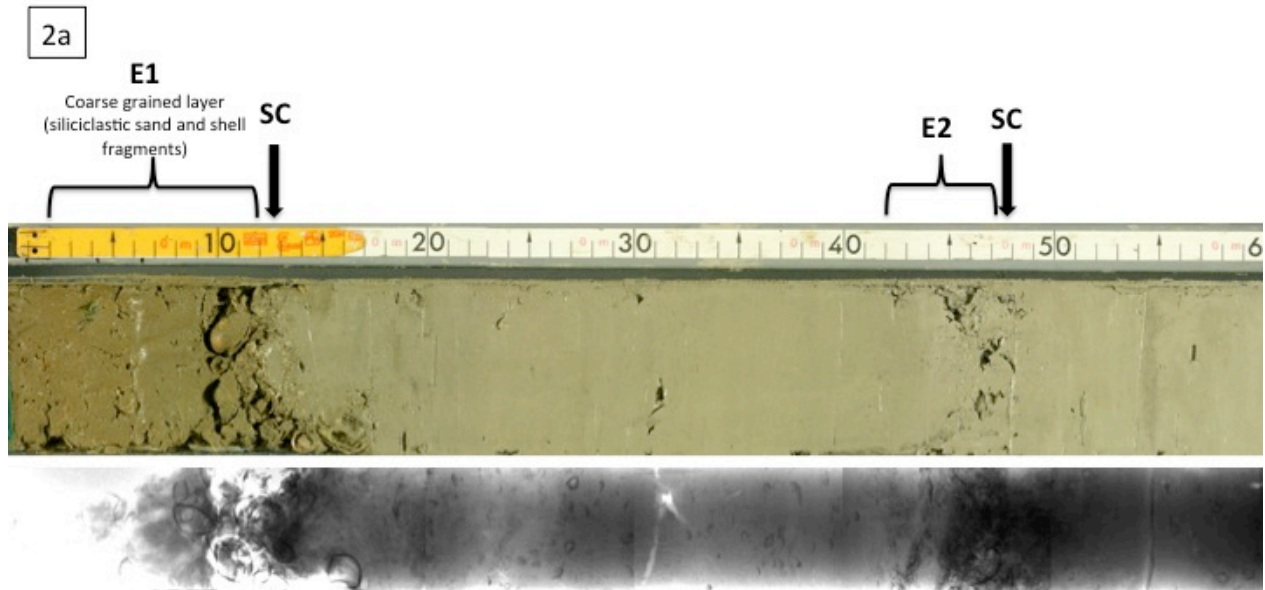
614

615 *Figures captions*
616
617
618
619
620
621
622
623

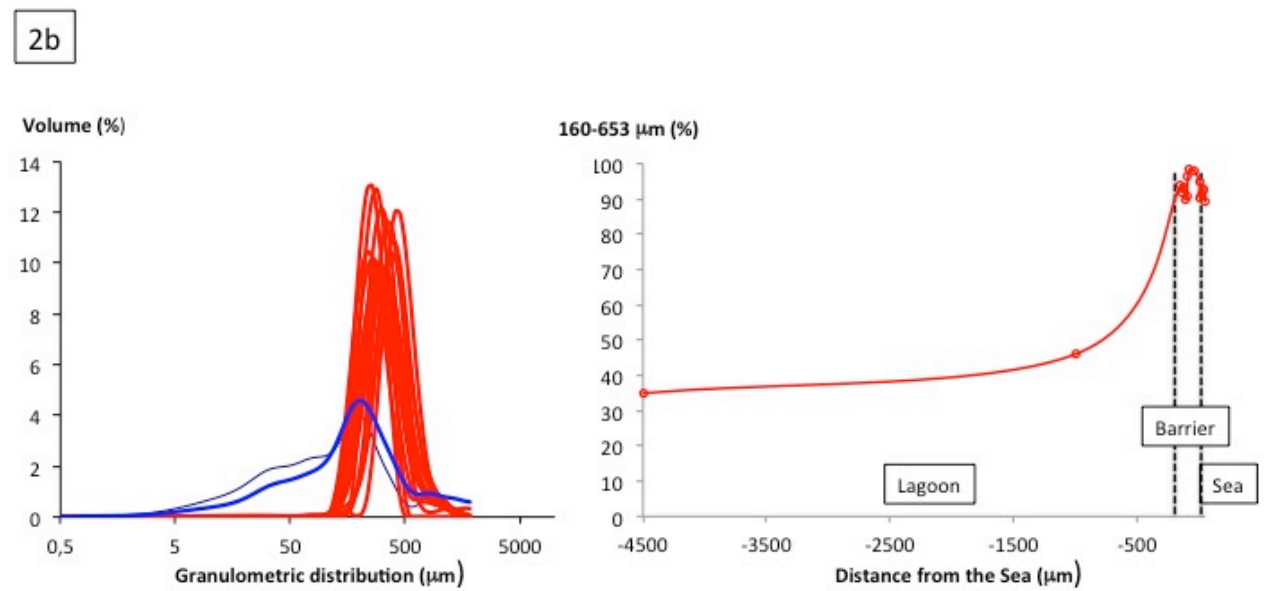


624
625
626
627
628 **Figure 1.** Map of the Mar Menor lagoon with localisation of the core MM2.
629
630

631
632
633



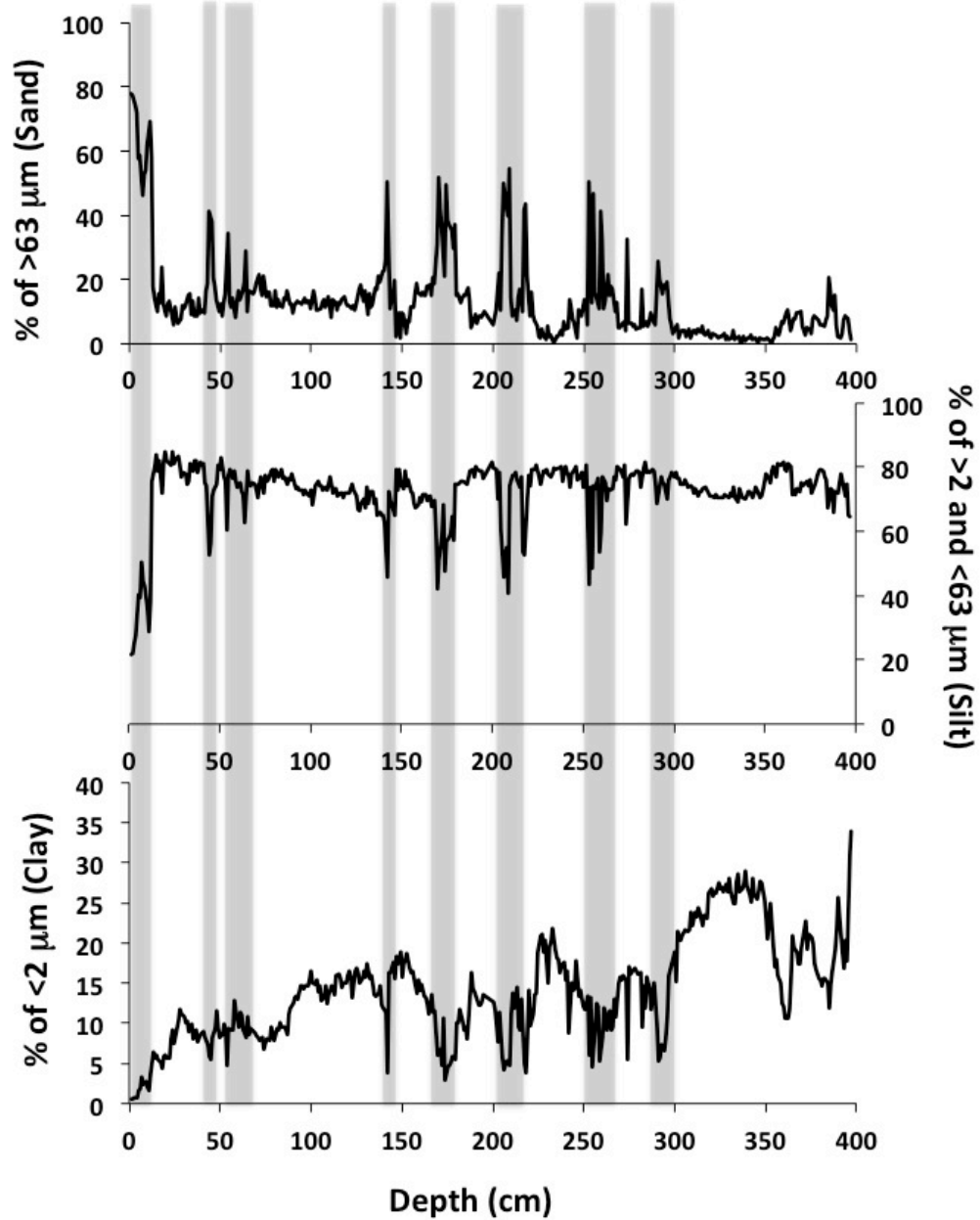
634



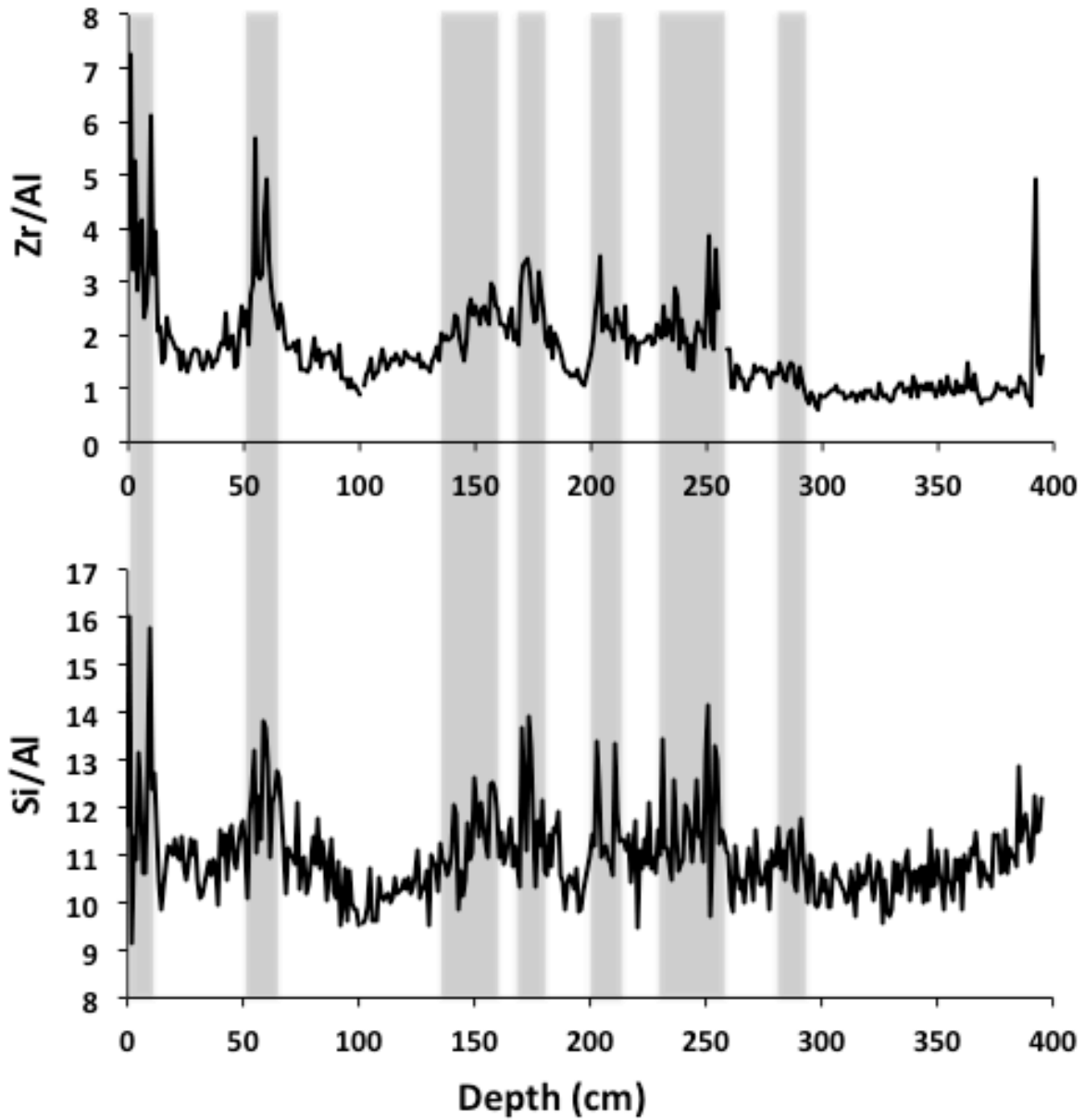
635

636

637 **Figure 2. a)** Photography and X-ray of the core MM2 (0 and 60 cm). Coarse grained layers are a
 638 mixture of siliciclastic sand and shell fragments. These layers have often sharp contacts (SC)
 639 with the clay and silt sediments below. **b)** Granulometric distribution of surface samples collected
 640 on a E-W transect from the Sea and the Barrier (red) to the lagoon (blue). Evolution of the 160-
 641 653 μm population from the sea to the lagoon in surface samples.



642
 643 **Figure 3.** Grain size population from the Mar Menor MM2 record with clay (<2 μm), silt (>2 and
 644 <63 μm) and sand fraction (>63μm). Shaded areas mark the main variations of the sand fraction.
 645



646

647

648

649 **Figure 4.** XRF records from the core MM2 with down-core variations of ratio Zr/Al and Si/Al.

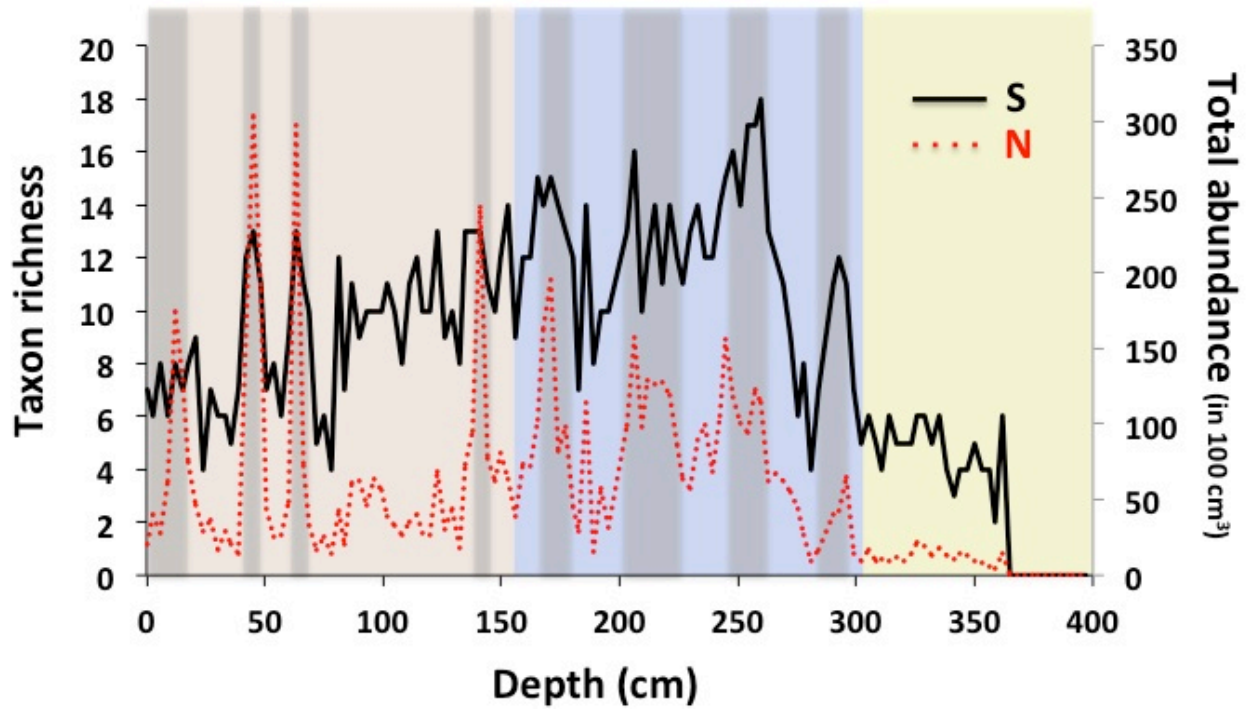
650 Shaded areas mark the main variations of Zr/Al and Si/Al.

651

652

653

654



655

656 **Figure 5.** Taxon richness (S) and total number of individuals (N) with depth from the core MM2.

657 Macro-fauna samples were taken at fixed volume (100 cm³). The different colour bands

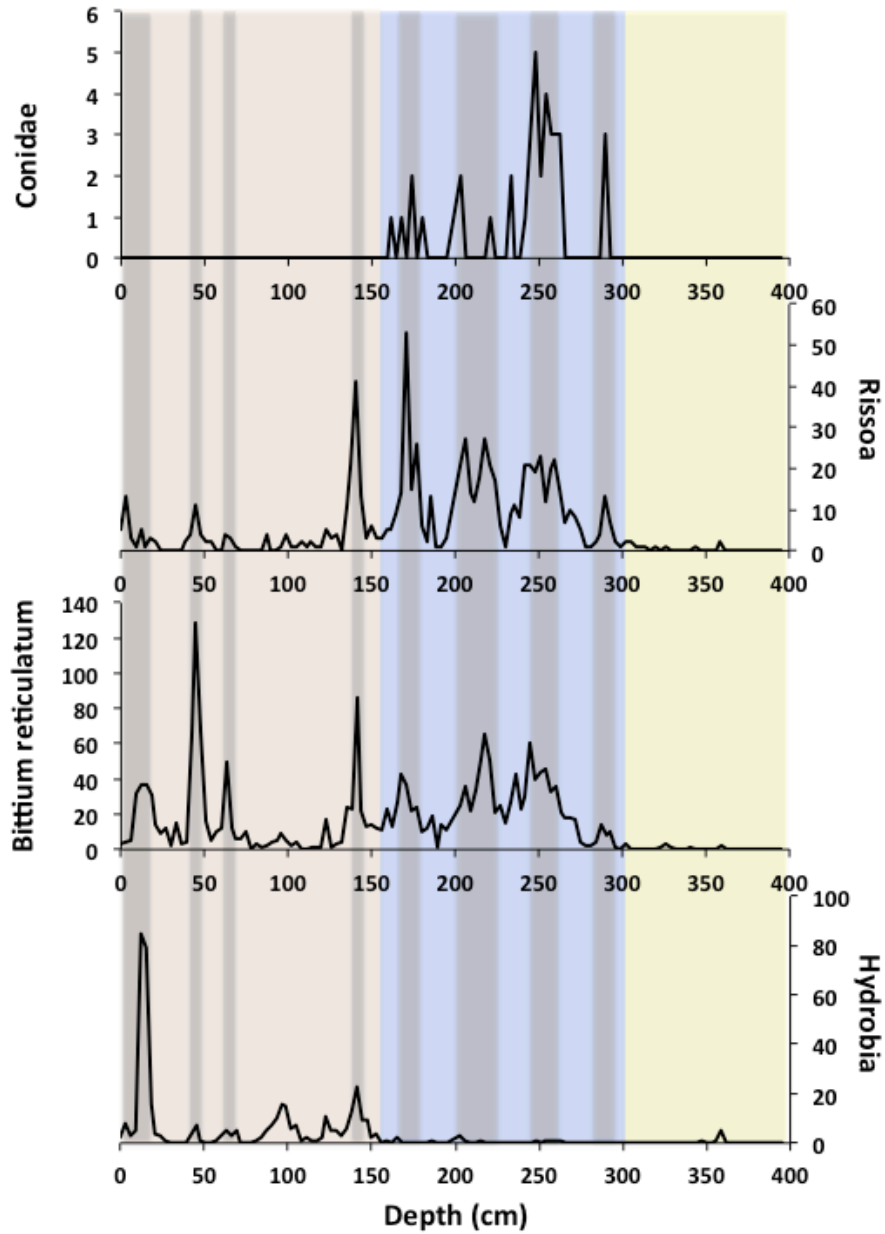
658 correspond to depths: azoic (yellow), under higher marine influence (blue) and under a

659 progressive isolation of the Mar Menor from the Mediterranean Sea (brown). The grey bands

660 correspond to punctual peaks in species richness, probably related to episodes of rupture of the

661 sandbar.

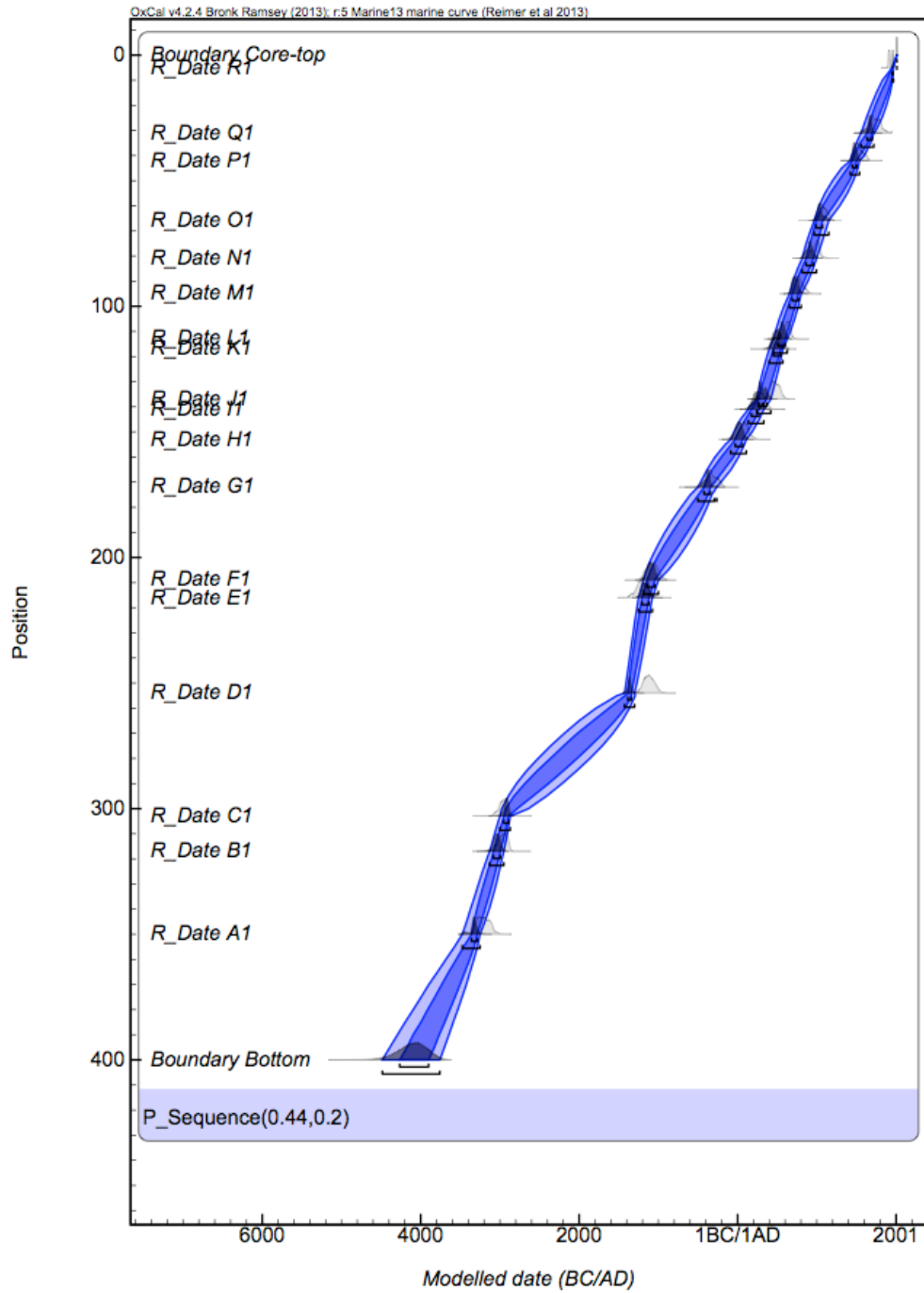
662



663
 664 **Figure 6.** Evolution of the abundance in mollusc population (number of individuals in 100 cm³)
 665 with depth: lagoonal specie (*Hydrobia acuta*); typical marine specie (*Conus ventricosus*:
 666 Conidae), marine influence (*Bittium Reticulatum* and *Pusillina lineolata*: Rissoa).

667

668

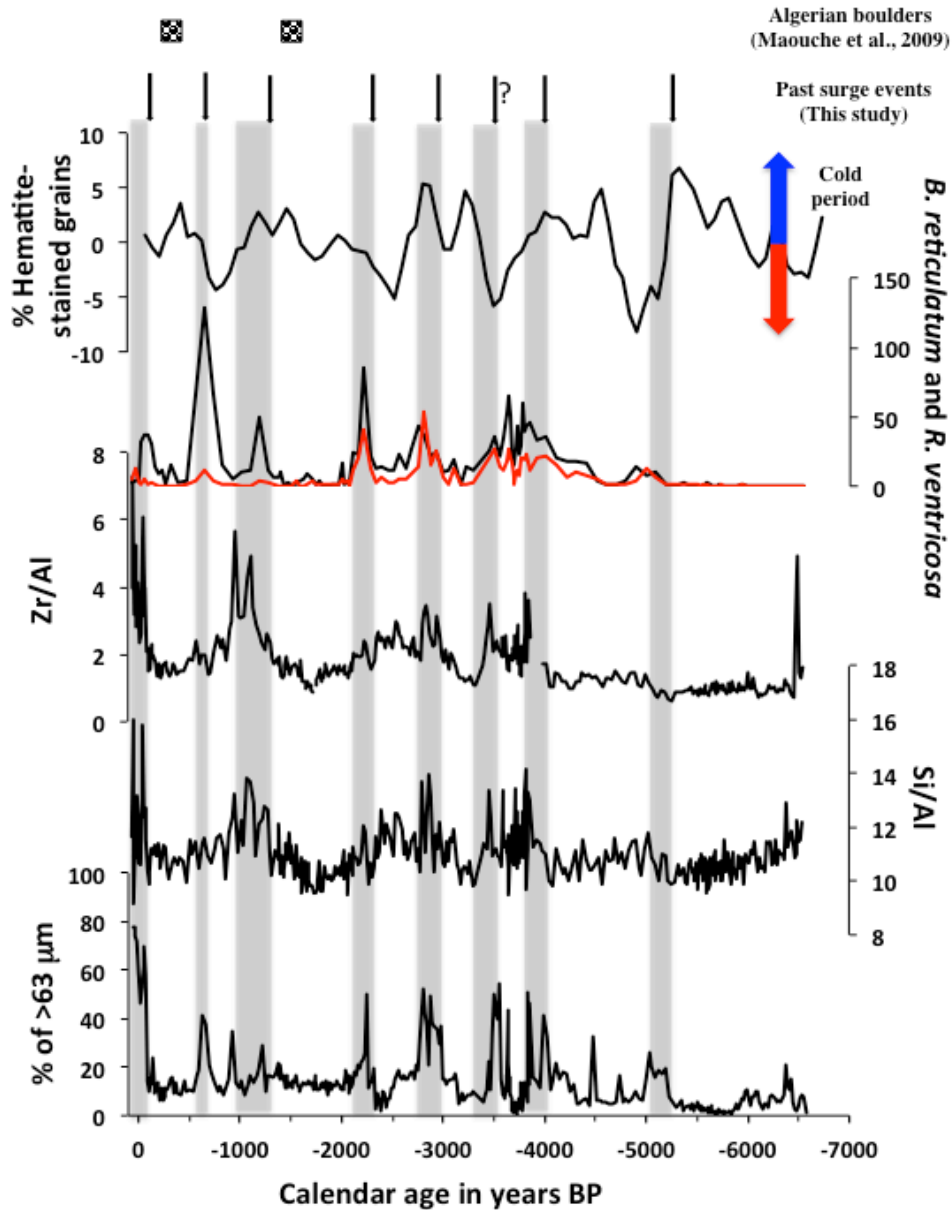


669

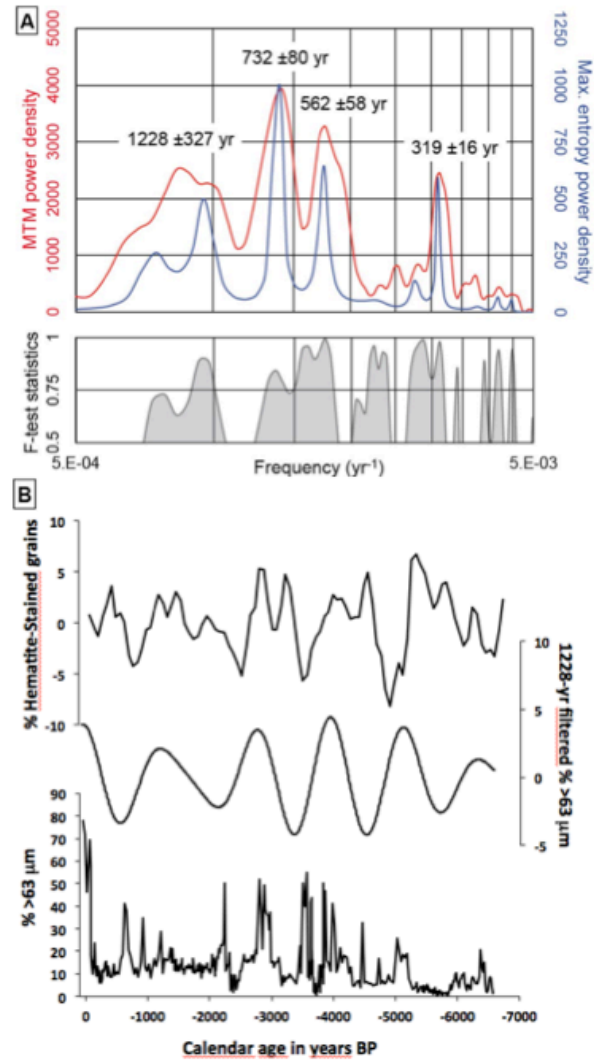
670 **Figure 7.** Age vs Depth for the core MM2. The Age model was calculated using OxCal 4 with 17

671 ¹⁴C dates.

672



673
 674
 675 **Figure 8.** Core MM2 with from bottom to top: Grain size (sand fraction); Si/Al and Zr/Al XRF
 676 ratio; number of *B. reticulatum* (Black line) and *R. Ventricosa* (Red line), % Hematite-stained
 677 grains (Bond et al., 1997, 2001), ages of Algerian boulders (Maouche et al., 2009). Grey bands
 678 are the past surge events.
 679



681

682 **Figure 9.** Time series analysis from the Mar Menor MM2 record. (A) Spectral analyses of the %
 683 of sand with AnalySeries v.2.0.8 (Paillard et al., 1996) by using the Multi-Taper method (linear
 684 trend removed, width.ndata product: 1.3; number of windows: 2) and the Maximum entropy
 685 method (linear trend removed, % of series: 40, number of lags: 133). (B) Comparison between
 686 the % Hematite-stained grains (Bond et al., 1997, 2001), the Gaussian filter on the % of sand for
 687 the 1228-yr period (frequency: 0.0008, bandwidth: 0.0002) and the sand fraction of the core
 688 MM2.

689